

# Theoretical and Experimental Study on Combustion Similarity for Different Size Diesel Engines

T.Chikahisa and T.Murayama

*Department of Mechanical Engineering  
Hokkaido University  
N13-W8, Sapporo 060  
Japan*

## ABSTRACT

The paper presents a theoretical study on combustion similarity in differently sized diesel engines and the partial experimental validation of the theory.

The theoretical consideration shows the possibility of combustion similarity, and the similarity conditions are identified. To verify the theoretical predictions, it was performed to observe similarity in fuel jet distribution in a model apparatus, and also comparisons of thermal efficiency, heat release rate, and emissions were made for engines varying from 260 to 400 mm in bore size. The results showed good agreement with the theory.

## INTRODUCTION

The purpose of this research is to determine the possibility of combustion similarities in differently sized diesel engines, and to propose conditions for realizing model experiments.

Diesel engine combustion has been widely investigated, but there is no theory of the size effects. Engine performance in large engines is estimated from experience, without the benefit of model experiments to perform fine optimization. Additionally, experimental data are considered unique for each engine, and are not applied to correlate with or predict performance under other conditions. Establishment of a theory of size effects will enable a correlation with the vast amount of independent data that is available, and so offer significant advantages for diesel engine research and design.

The authors have reported the theory of this investigation in the JSME International Journal(1). The present report briefly describes the theoretical considerations, and details experimental results to verify the theory.

The symposium on "Size effect and similarity theory on diesel engine combustion", Tokyo, March 1982, is of direct relevance to combustion similarity in diesel engines (2). The symposium covered similarities in fuel spray, air motion, heat transfer, combustion, lubrication, and engine performance, and the main conclusion of the symposium was that the establishment of a similarity theory would be impossible. However, the evaluation of the data presented at the symposium may be expanded with the present theory, because the dis-

cussion then was based on simple comparisons of experimental data without nondimensional treatment.

The detailed survey of research on combustion similarity is in the reference (1).

## DISCUSSION AND DEVELOPMENT OF SIMILARITY THEORY

Combustion is considered similar when flow pattern, fuel spray distribution, ignition points, and heat release distribution are similar for two different engines. For the establishment of similarity, it is sufficient to show that the fundamental equations of change and both the boundary and initial conditions are correspondent in nondimensional forms between the two compared engines.

In the present research, the following assumptions are made:

(1) spray droplets are very small, and evaporate rapidly in near critical pressure of the fuel, so that the fuel spray can be treated as a gas jet,

(2) combustion takes place diffusively, and the reaction rate is controlled by the mixing of fuel and air,

(3) the working fluid in the cylinder can be treated as a perfect gas which has average properties during a cycle.

With these assumptions, the correspondence of fundamental equations and the initial and boundary conditions are discussed in the following.

### Similarity of Fundamental Equations of Change

The fundamental equations of continuity, motion, and energy are expressed in vector form (3)(1):

$$\left. \begin{aligned} \frac{D\rho}{Dt} &= -\rho(\nabla \cdot \mathbf{u}) \\ \rho \frac{D\mathbf{u}}{Dt} &= \mu_t \nabla^2 \mathbf{u} - \nabla p \\ \rho c_p \frac{DT}{Dt} &= k_t \nabla^2 T + \frac{Dp}{Dt} + \left( \frac{DQ}{Dt} \right)_c \end{aligned} \right\} \quad (1)$$

here  $\mu_t$  and  $k_t$  are the eddy viscosity and eddy thermal conductivity, and  $(DQ/Dt)_c$  is the generated heat of combustion.

The following parameters are nondimensionalized by dividing with the 0 suffix reference values:

$$x^* \equiv x/x_0, \quad t^* \equiv t/t_0$$

$$\begin{aligned}
 u^* &\equiv u/u_0, \quad \rho^* \equiv \rho/\rho_0 \\
 T^* &\equiv T/T_0, \quad p \equiv p(t) + \Delta p(t, x) \\
 p^*(t) &\equiv p(t)/p_0, \quad \Delta p^* \equiv \Delta p/(\rho_0 u_0^2)
 \end{aligned}$$

where  $p_0$ ,  $T_0$ , and  $\rho_0$  are the cylinder gas values at the piston position of bottom dead center. The pressure  $p$  is defined as the sum of  $p(t)$ , mean pressure in the cylinder, and  $\Delta p(t, x)$ , spatial variation from the mean value in the cylinder. The  $p(t)$  is a function of time, while  $\Delta p(t, x)$  is a function of both time and position. The two parameters are nondimensionalized by  $p_0$  and  $\rho_0 u_0^2$  respectively. The reference time,  $t_0$ , is defined as  $t_0 \equiv x_0/u_0$ . Substitution of these parameters into Eq.(1) gives the following nondimensional equation of change:

$$\left. \begin{aligned}
 \frac{D^* \rho^*}{D^* t^*} &= -\rho^* (\nabla^* \cdot u^*) \\
 \rho^* \frac{D^* u^*}{D^* t^*} &= \frac{1}{Re} \nabla^{*2} u^* - \nabla^* \Delta p^* \\
 \rho^* \frac{D^* T^*}{D^* t^*} &= \frac{1}{Re \cdot Pr} \nabla^{*2} T^* + \frac{\kappa - 1}{\kappa} \frac{dp^*(t)}{dt^*} \\
 &+ \frac{Br}{Pr} \frac{D^* \Delta p^*}{D^* t^*} + \frac{Hu}{c_p \cdot T_0} \left( \rho^* \frac{D^* F_i}{D^* t^*} \right)_c
 \end{aligned} \right\} (2)$$

$$\therefore Re \equiv \frac{\rho_0 x_0 u_0}{\mu_t}, \quad Pr \equiv \frac{c_p \mu_t}{k_t}, \quad Br \equiv \frac{\mu_t}{k_t} \frac{u_0^2}{T_0}$$

in which  $\kappa$  is the specific heat ratio,  $F_i$  is the local mass fraction of the fuel,  $H_u$  is its lower heating value, and  $c_p$  is the mean specific heat of the cylinder gas. The  $Re$ ,  $Pr$ , and  $Br$  are the Reynolds number, Prandtl number, and Brinkman number defined by eddy viscosity and eddy thermal conductivity.

The term with ( )<sub>c</sub> denotes the chemical change of the fuel mass, and a solution requires the following additional equation for continuity of the chemical species:

$$\rho^* \frac{D^* F_i}{D^* t^*} = \rho^* \frac{1}{Re \cdot Sc} \nabla^{*2} F_i + \left( \rho^* \frac{dF_i}{dt^*} \right)_c \quad (3)$$

$$\therefore Sc \equiv \mu_t / (D_{it} \cdot \rho_0)$$

where  $Sc$  denotes Schmidt number, and  $D_{it}$  is the eddy diffusivity.

Here, we rewrite the chemical reaction term in the second term of the right-hand side in Eq. (3) to  $S_i$ , in which  $i=1$  corresponds to the fuel, 2 for air, and 3 for the combustion products. Assuming the combustion rate to be controlled by the mixing speed of fuel and air, we obtain the following equations;

$$\left. \begin{aligned}
 S_2 &= AF_0 \cdot S_1 \\
 S_3 &= -(S_1 + S_2) = -S_1(1 + AF_0) \\
 F_1 \cdot F_2 &= 0
 \end{aligned} \right\} (4)$$

where  $AF_0$  denotes the stoichiometric air-fuel ratio. The state equation is expressed in nondimensional form as:

$$p^* = \rho^* T^* \quad (5)$$

The above equations are a complete set of fun-

damental equations. A solution of this series of equations expresses the complex flow and combustion state in the cylinder. The equations include six nondimensional coefficients:  $Re$ ,  $Pr$ ,  $Br$ ,  $Sc$ ,  $AF_0$ , and  $H_u/(c_p T_0)$ . To establish similarity, all of the six coefficients must coincide for different engines.

This condition shows that the fuels must have the same  $AF_0$  and  $H_u/c_p T_0$ . This can be achieved by using the same kind of fuel for the two engines. Additionally, as many petroleum fuels have similar C/H ratios and  $H_u$  (1), this condition can be established without major difficulty.

For the Brinkman number,  $Br$ , the  $\Delta p$  term in the energy equation, which is a small pressure variation, does not affect the  $T$  and  $\rho$  distributions perceptively, and the flow change due to ignoring the  $\Delta p$  term in the energy equation can be assumed to be negligible. Therefore, the third term on the right-hand side of the energy equation in Eq.(2), which contains  $Br$ , can be omitted.

As a result, the condition necessary for the similarity is that the three diffusivity coefficients,  $Re$ ,  $Pr$ , and  $Sc$ , are similar for different engines.

#### Diffusivity Coefficients in Turbulent Flow Field

When turbulent flow is dominant, the following relationship is available (3):

$$Pr \approx Sc \approx \text{const.} \quad (6)$$

Here  $Re$  is the only parameter necessary for similarity in equations of change.

The definitions of Reynolds stress  $\tau$  and eddy viscosity gives

$$\tau = -\mu_t \frac{\partial u}{\partial y} \quad (7)$$

and according to von Karman (3), the  $\tau$  is

$$\tau = -\rho K_2^2 \left| \frac{(du/dy)^3}{(d^2u/dy^2)^2} \right| \frac{du}{dy} \quad (8)$$

$$\therefore K_2 \approx 0.36 \sim 0.40$$

By combining Eqs. (7) and (8), we obtain

$$Re = \frac{\rho_0 x_0 u_0}{\mu_t} = \frac{1}{K_2^2} \left[ \rho^* \left| \frac{(du^*/dy^*)^3}{(d^2u^*/dy^{*2})^2} \right| \right]^{-1} \quad (9)$$

Equation (9) indicates that the Reynolds number defined with eddy viscosity is a function of other nondimensional parameters, and these are consistent for different engines. This implies that the local Reynolds number is self-consistent for different engine sizes, when the other similarity conditions are satisfied.

The equation of von Karman is considered to apply only for the region close to the wall (4). However, the same result is obtained with the Prandtl mixing length theory for wall surface flow, eddy viscosity for flow through parallel plates, and the eddy viscosity of Tollmien's theory for free jets (5). This implies that the above deductions for the Reynolds number are acceptable. Therefore, due to the self-consistent Reynolds number, the flow in a turbulent flow field apparently becomes similar, independent of size.

In conclusion, this shows that all of the

three diffusivity coefficients are self-consistent for different engine sizes. Hence, when fuels have the same Afo and Hu/cpTo, the fundamental equations are correspondent.

#### Boundary and Initial Conditions

To establish similarity, correspondence of initial and boundary conditions as well as the fundamental equations must be satisfied. A primary boundary condition for similarity is the consistency in the combustion chamber configuration between two engines. This means consistency must be maintained in piston shape, compression ratio, valve location, and so forth. Nozzle location, diameter and number of nozzle holes, and injection direction must also be similar and proportional to the engine size.

Additionally, the nondimensional piston speed must be equal. With  $r_c$  as the crank radius,  $l$  the connecting rod length,  $\theta$  the crank angle, and  $n$  the engine speed, the nondimensional piston speed,  $u_p^*$ , is: (6)

$$u_p^* \equiv \frac{u_p}{u_0} = \frac{r_c}{u_0} \left( \sin \theta + \frac{r_c}{2l} \sin 2\theta \right) \cdot \frac{n\pi}{30} \quad (10)$$

Assigning the cylinder bore  $D$  to the reference length  $x_0$ , Eq.(10) for the similarity condition of  $u_p^*$  becomes the following, since  $r_c$  is proportional to  $D$ .

$$\frac{nD}{60 u_0} = \text{const.} \quad (11)$$

Here, const. means that the value is the same for two different engines, and it does not need to be constant with time. According to Eq. (11), crank angle is also the same for non-dimensional time,  $t^*$ , as:

$$\theta = \frac{n\pi}{30} t = \frac{Dn\pi}{30u_0} t^* = \text{const.} \quad (12)$$

The approximate similarity conditions at the nozzle exit are satisfied by using the mean nozzle exit velocity of the fuel for the reference velocity,  $u_0$ , and making the nozzle exit diameter,  $d_n$ , proportional to the cylinder bore,  $D$ . Here, the  $u_0$  is calculated by:

$$u_0 \equiv \frac{4m_f}{\rho_f \pi d_n^2 \Delta \theta_{inj} N_z} \cdot \frac{d\theta}{dt} = \frac{4m_f \cdot n}{30 \rho_f d_n^2 \Delta \theta_{inj} N_z} \quad (13)$$

where  $m_f$  is the total amount of injected fuel, and  $\Delta \theta_{inj}$  is the injection duration.

To satisfy the similarity condition in the nozzle exit at any instance, the following equation for fuel injection rate is established:

$$\begin{aligned} u_n^* \equiv \frac{u_n}{u_0} &= \frac{1}{u_0} \cdot \frac{4\dot{m}_f(\theta)}{\rho_f \pi d_n^2 N_z} \cdot \frac{d\theta}{dt} \\ &= \frac{\dot{m}_f(\theta)}{m_f} \cdot \Delta \theta_{inj} = \text{const.} \end{aligned} \quad (14)$$

where  $\dot{m}_f(\theta)$  is the injection rate for the unit crank angle radian.

As another initial condition, there is an in-cylinder state at the bottom dead center before compression,  $p_0$ ,  $\rho_0$ , and  $T_0$ . Since these

parameters are selected as the reference values, the condition is automatically satisfied.

The swirl ratio is one of the initial conditions, too. If the swirl flow is assumed to be rigid-body rotation, the similarity condition of  $u^*$  at radius  $r$  from the center is

$$u^* = \frac{r\omega_s}{u_0} = \frac{Dr^*}{u_0} \cdot SR \cdot \frac{n\pi}{30} \propto r^* SR = \text{const.} \quad (15)$$

where  $SR$  is the swirl ratio, and  $\omega_s$  is its angular velocity. Equation (15) shows that the swirl ratio should be equal for two engines.

In addition to the above conditions, the ignition lag in the radians of crank angle must correspond. This can be controlled by, for example, ignition improvement additives.

Thus, this section concludes that similarity of fundamental equations and initial and boundary conditions can be established, and the conditions necessary for the similarity were identified.

Similarity conditions in fuel spray and heat transfer are detailed in the previous report (1), together with notes on the execution of model experiments.

#### EXPERIMENTAL VALIDATION OF THE SIMILARITY THEORY

##### Similarity in Fuel Jet Development, and the Effect of Reynolds Number

To confirm the effect of Reynolds numbers, fuel jet development was compared in model experiments. Air motion in the cylinders of large engines is almost quiescent, and injected fuel evaporates in a very short time compared with the piston movement, behaving as a gas jet. The pressure in the cylinder does not affect the development of the gas jet, when density differences between liquid spray and gas jet are compensated to the same momentum by increasing the nozzle diameter(7). This would seem to allow model experiments at ambient pressure.

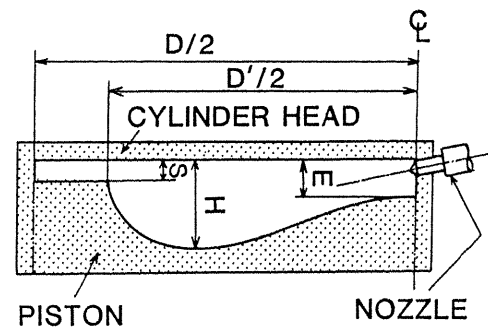


Fig.1 Model chamber for jet observation

Table 1 Specification of the apparatus (unit: mm)

TYPE	D	D'	H	S	E	d <sub>n</sub>
I	400	316	42	11	20	2.2
II	260	204	27	7	13	1.4
III	125	100	13	3.4	6.3	0.7

Experimental apparatus. Fig.1 shows the experimental apparatus, which consists of a two dimensional combustion chamber and a CO<sub>2</sub> gas injector. The chamber is placed in a Schlieren photography apparatus, and the observation ports are open to the atmosphere. The nozzle hole diameter was set proportional to the bore as shown in table 1.

The CO<sub>2</sub> gas was injected from the nozzle at 0.6 MPa back pressure, which is high enough to cause choking, and operated by a modified gas sampling valve. Here, nondimensional time was defined as  $t^* = t \cdot u_0 / d_n$ , and the nozzle diameter was used for the Reynolds number.

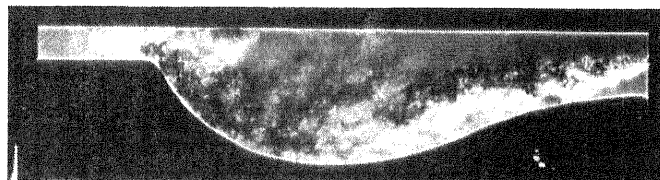
Experimental results. Fig.2 shows a comparison of Schlieren photographs for the three different size models at the same nondimensional time. The pictures are at the same magnification to make comparisons easier. The gas jets show a very similar shape although the Reynolds numbers vary by about three times. Particularly the reflection at the wall and the jet front penetrating into the top clearance are very similar.

This indicates that the fuel jets develop similarly in different size engines and that they are independent of the Reynolds numbers, implying that the theoretical considerations proposed here are valid.

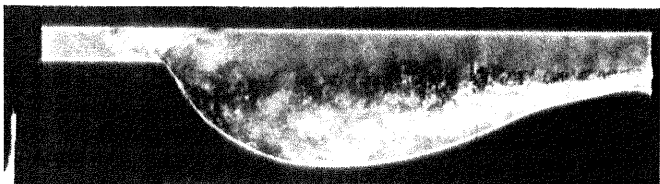
#### Experimental Comparison on Heat Release Rate and Emissions for Different Size Engines

In this section similarity in the rate of heat release, NO<sub>x</sub> emissions, and indicated thermal efficiency are compared for three differently sized engines. The theory directly considers the combustion rate, and the rate of heat release is direct indication of the fit of the theory.

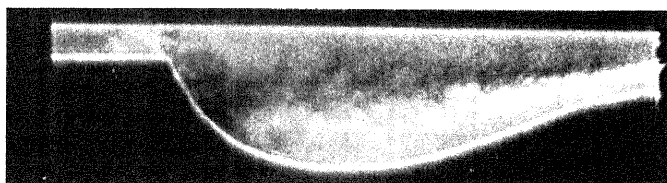
Experimental apparatus. Engines with 260 to



D=400mm, Re=40000, t=3.6ms



D=260mm, Re=25500, t=2.2ms



D=125mm, Re=12700, t=1.0ms

Fig.2 Comparison of gas jet development for the different size model chambers;  $t^* = 230$

400 mm bore diameter were used in the experiment as shown in table 2. They are selected to have relatively similar engine configurations. Engine "B" has a nozzle with 9 holes instead of the 10 in engines "A" and "C", and the total nozzle hole area relative to the cylinder sectional area was similar in all three engines.

To eliminate the dilution effect by the air, NO<sub>x</sub> emissions were compared with an emission index, i.e. NO<sub>x</sub> weight relative to the consumed fuel weight. All the data were corrected to have the same injection start timing at 10 deg. BTDC (8).

Experimental results. Fig.3 shows peak values of the diffusive combustion and their positions plotted with  $nD/60u_0$ . Data for the three different indicated mean effective pressures (IMEP;  $P_i$  in the figure) are included. The rate of heat release is expressed in %/CA relative to the total integrated heat release.

It is seen that all the data arranges on curves for the three different IMEP's, which closely match the theoretical prediction of air entrainment changes in sprays for  $nD/60u_0$  (7). The data with engine "A" for constant and also variable engine speeds,  $\Delta$  and  $\nabla$ , fall on the predicted theoretical curves. It is important to note that the data for different size engines all match the theoretical curves. This indicates the possibility of combustion similarity for different size engines.

Fig.4 is a comparison of rate of heat release for engines "A", "B", and "C" at the IMEP ( $P_i$ ) of 1.9 MPa. The parameters of  $nD/60u_0$  for engine "A" and "B" are about the same, while engine "C" has smaller values. The rate of heat release is very similar for engines "A" and "B", particularly in the diffusive combustion part. The premixed combustion part is slightly different for the two engines due to different ignition lags. The coincidence in the diffusive combustion rate of the two differently sized engines indicates the applicability of the present similarity theory.

The combustion rate of engine "C" is higher and terminates earlier than for engine "A" and "B", due to the smaller  $nD/60u_0$  of engine "C".

Table 2. Engine specification and test conditions

ENGINE	A		B	C		
BORE D mm	260		320	400		
STROKE/D	1.06		1.13	1.15		
D' / D	0.788		.788	0.858		
H/D x10 <sup>2</sup>	7.88		7.19	7.25		
NO.OF CYL.	6		18	3		
COMP.R. $\epsilon$	12.7		13.3	14.7	11.4	
d n mm	0.43	0.42	0.56	0.75		
HOLES N z	10		10	9	10	
n rpm	1000	VAR.	1000	750	514	
INJ.TIMING	-10 ° CA		-14	-10		
SYMBOL	$\Delta$	$\nabla$	$\triangleright$	$\circ$	$\square$	$\diamond$

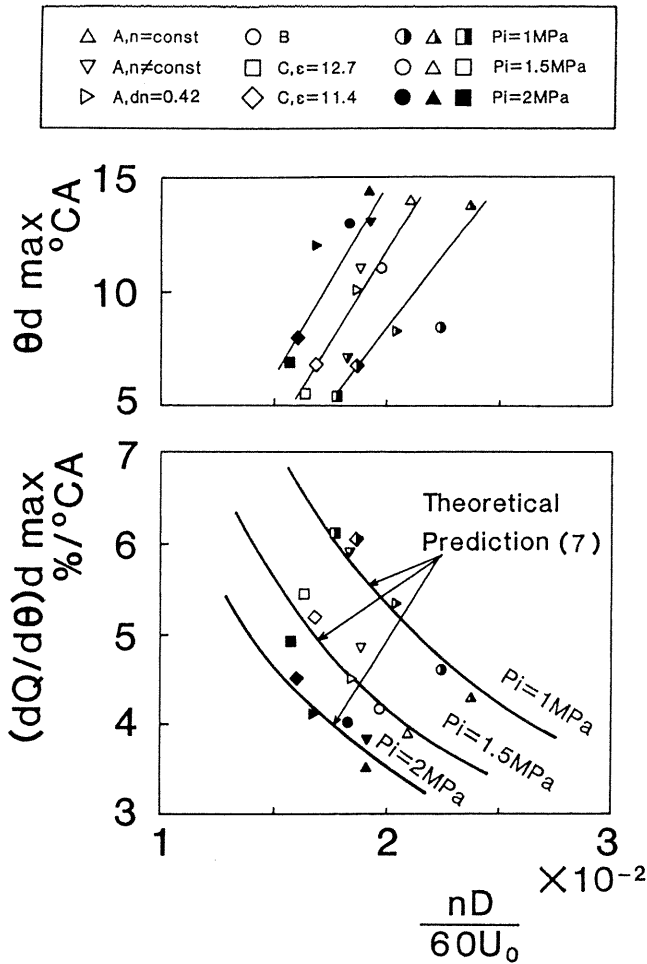


Fig.3 Peak of the diffusive combustion rate

The present theory suggests that decreases in engine speed and increases in injection speed have equal weight and are integrated as a parameter of  $nD/60U_0$ . If the  $nD/60U_0$  of "C" is equal to the other two engines, the combustion rate would also become equal. This becomes understandable with the following comparison.

Fig.5 shows the rates of heat release for two different  $nD/60U_0$ 's with engine "A" and one for engine "C". It is seen that the combustion rate increases and the duration decreases as the  $nD/60U_0$  decreases in the same engine. It may therefore be expected that the combustion of engine "A" and "C" becomes similar, if the  $nD/60U_0$  of engine "A" decreases to the value of engine "C".

Next, comparisons were made of NOx emissions and the indicated thermal efficiency. The result is shown in Fig.6, where the data are expressed relative to the reference value. The reference values,  $\eta_{io}$  and  $NO_{x0}$ , are the value at IMEP of 1.5MPa with engine "A" in 1000rpm, i.e. symbol  $\Delta$ . The NOx emission changes similarly with diffusive combustion shown in Fig.3 except for the data of engine "B". This may be attributed to the lower premixed combustion of engine "B" due to the shorter ignition lag.

The NOx emission is controlled by chemical reactions rather than mixing speed, so together with the  $nD/60U_0$  the time factor is also important. When time factor is not significant as the present results, NOx emission will also tend to be similar

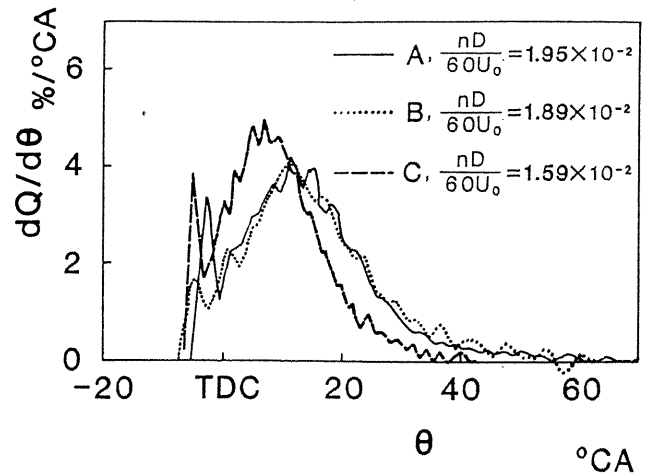


Fig.4 Comparison of heat release curves at IMEP of 1.9MPa. The data for engine "A" corresponds roughly to  $\nabla$ , "B" to  $\bullet$ , and "C" to  $\blacksquare$  in Fig.3.

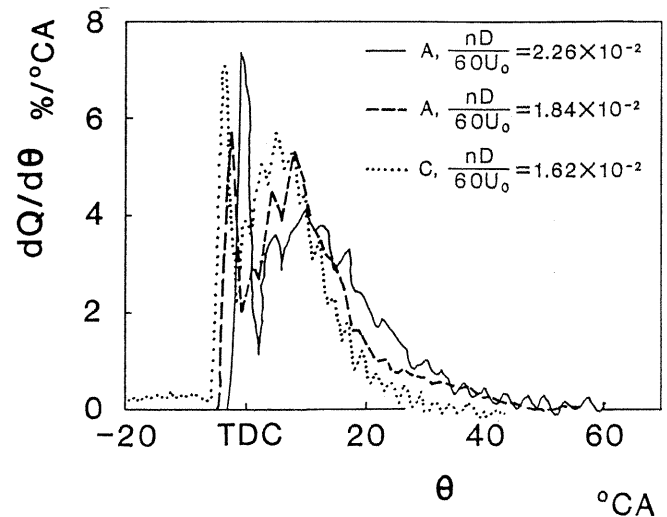


Fig.5 Changes in heat release curves for the  $nD/60U_0$ ; IMEP is 1.4 MPa.

for different size engines. Even if the time factor is important, it is possible to predict NOx emission of different size engines by taking the factor into account, because the temperature and mixture distribution are similar.

The Indicated thermal efficiency should be more directly related to the rate of heat release than NOx. It was calculated from a direct integration of indicator diagrams and injected fuel amounts. Cooling loss and degree of constant volume of combustion affect the indicated thermal efficiency. In Fig.6 it is seen that data at the same IMEP arrange linearly, and the declinations of the lines are different depending on the IMEP. The data with symbol  $\triangleright$  are the exception. This may be caused by some error in the indicator diagram. As the IMEP increases the inclination of the line decreases, and smaller  $nD/60U_0$  gives larger indicated thermal efficiencies. This appears to be caused by improved degree of constant volume of combustion due to shorter combustion durations for smaller  $nD/60U_0$ . When IMEP is low, 1MPa, smaller  $nD/60U_0$  gives lower thermal efficiency. This seems to be partly due to larger cooling loss and very early combustion start be-

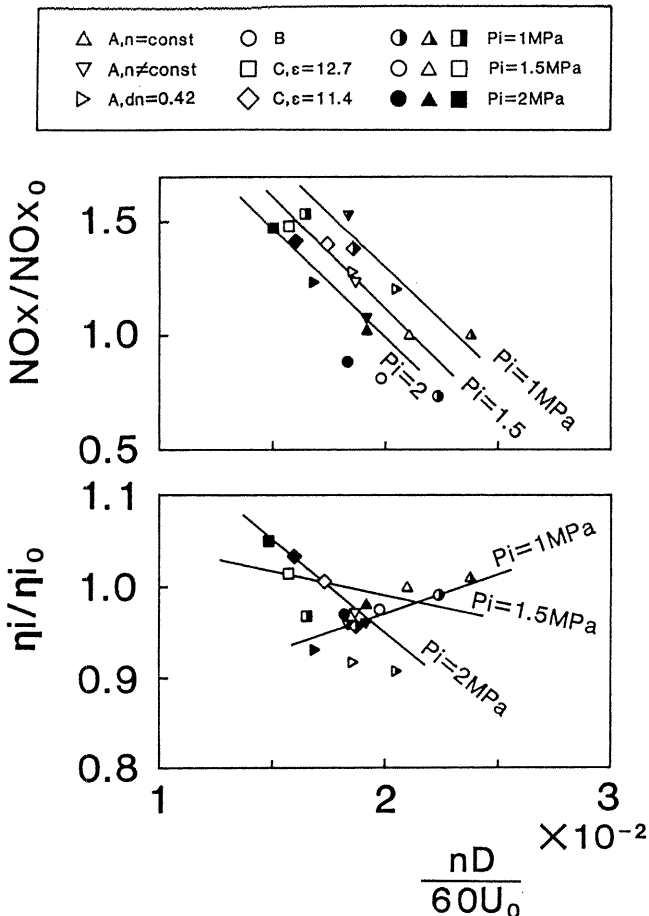


Fig.6 NO<sub>x</sub> emission and indicated mean effective pressure,  $\eta_i$ .

cause of the very short combustion with a high peak of premixed combustion. Over-penetration of the spray due to smaller  $nD/60U_0$  may be another reason at low boost pressure in partial load.

As rate of heat release is similar for different size engines, it will be possible to predict the indicated thermal efficiency for differently sized engines from the cooling loss and degree of constant volume of combustion of the heat release curves.

The data in the present experiments all show good agreement with the predictions of the theory, although more work is necessary to fully validate the theory.

#### CONCLUSIONS

1. A theoretical investigation has shown that it is possible to establish combustion similarity for different size diesel engines. The theory predicts that useful model-experiments are possible.

2. The similarity conditions identified involve engine configuration, injection system, fuel properties, swirl ratio, engine speed, and ignition lag. The most important factors among these are the nozzle diameter,  $nD/60U_0$ , and ignition lag.

3. Model experiments showed similar fuel jet development for different size engines. The results indicate that Reynolds numbers have little effect on the phenomena in engines.

4. Experimental results with real engines with bore sizes from 260 to 400 mm showed good agreement with the theoretical predictions.

#### NOMENCLATURE

A<sub>F0</sub>: stoichiometric air-fuel ratio  
 D: bore, m  
 D<sub>it</sub>: eddy diffusivity, m<sup>2</sup>/s  
 d<sub>n</sub>: nozzle diameter, m  
 F<sub>i</sub>: mass fraction of chemical species  
 H<sub>u</sub>: lower heating value of fuel, J/kg  
 k<sub>t</sub>: eddy thermal conductivity, W/(m·K)  
 m<sub>f</sub>: total injected fuel quantity, kg  
 N<sub>z</sub>: number of nozzle holes  
 n: engine speed, rpm  
 p: pressure, Pa  
 P<sub>i</sub>: indicated mean effective pressure, MPa  
 S<sub>i</sub>: chemical reaction term  
 SR: swirl ratio  
 T: temperature, K  
 t: time, s  
 u: velocity, m/s  
 u<sub>0</sub>: average nozzle exit velocity, m/s  
 ε: compression ratio  
 θ: crank angle, rad  
 κ: specific heat ratio  
 ρ: density, kg/m<sup>3</sup>  
 μ<sub>t</sub>: eddy viscosity, kg/(m·s)  
 Subscripts  
 a: air  
 f: fuel  
 0: reference value  
 Superscript  
 \*: non-dimensional value

#### ACKNOWLEDGMENT

The authors wish to thank Mr. Tateo Nagai and Dr. Masayoshi Kawakami of Niigata Engineering Co., Ltd. for their cooperation on the experimental data supply with real engines. Appreciation is extended to Mr. Hitoshi Ouchi and Mr. Toshiyuki Fukuda, students in our laboratory, for their help in the model experiment.

#### REFERENCES

- Chikahisa, T., and Murayama, T., "Theory on combustion similarity for different-sized diesel engines", JSME Int. J., Vol.33, No.2, 1990
- JSAE Diesel Committee, Text for the symposium on size effect and similarity theory on diesel engine combustion, pp 1-73, 1982 (in Japanese)
- Bird, R., Stewart, W., and Lightfoot, E., Transport Phenomena, John Wiley & Sons, New York, p 322, 379, 160, 1960
- Launder, B. and Spalding, D., Mathematical Models of Turbulence, Academic Press, London, p11, 1972
- Schlichting, H., Boundary Layer Theory, McGraw-Hill, New York, p587, 602, 606, 735, 747, 1979
- Miyamoto, N., and Murayama, T., "Discussions on the Calculating Techniques of the Rate of Heat Release and Burning Rate in Diesel Engines and Influencing Error Factors", J. Int. Comb. Engine, Vol.18, NO. 224, pp.9-22, 1979 (in Japanese)
- Chikahisa, T., Murayama, T., and Yoneno, N., "Theoretical study on optimum conditions for fuel injection system and swirl flow in DI diesel engines", Proc. of 8th IC Engine Symposium in Japan, pp7-12, 1990 (in Japanese)
- Nagai, T., Kawakami, M., and Okeya, T., "Investigation on reducing NO<sub>x</sub> emission of medium-speed diesel engines", 18th CIMAC, vol.1, pp241-260, 1989